

Figure Legends for Supplemental Data

Figure S1. Interference-free transitions. Transition peak area percentages over 90 injections are shown for different peptides derived from protein biomarker candidates. The library bar indicates the fragment intensity percentage from the shotgun data. Peptides show unchanged peak area percentages, demonstrating interference-free properties of the selected transitions. TRML1-derived peptides showed strong variations regarding the transition peak area percentage due to very low peak intensity and, therefore, TRML1 was excluded from the panel of biomarker candidates.

Figure S2. The workflow of MRM assay development. The shotgun analysis revealed 96 proteins significantly regulated in serum samples from melanoma patients in comparison to healthy donors, as well as in melanoma with high tumor load (low TL) in comparison to low TL. By applying the selection criteria listed in the upper part of the figure and using the skyline software we ended up with the final MRM dynamic method consisting of 58 proteins, 92 peptides, and 276 transitions. Proteins included in the final MRM method are listed in the lower part of the figure.

Figure S3. Evaluation of analytical parameters of MRM analysis. A - Reproducibility of LC-MS measurements for 89 peptides. Coefficients of variation (CVs) were calculated based on triplicate injections and plotted against their average RT. Notably, early eluting peptides (<8 min) showed unusually high CVs. **B - Assay linearity.** The calibration curve of non-human standard synthetic peptide (VLETKSLYVR) spiked into digested and depleted serum sample of a healthy donor is shown. The x axis shows the peptide amount injected on column and in the y axis the absolute peak area of the peptide is plotted. **C - Depletion efficiency of Pierce top 12 spin columns.** Depletion efficiency was determined by comparing abundances of nine

proteins before and after depletion in samples from healthy donors as well as in melanoma samples with high tumor load (high TL). Peak areas were compared on protein level, normalizing the results to those of the standard peptides and to the serum volume. Depletion proved to be sample-independent and highly efficient (average ~84%) with low variation (average CV 4.2%). **D - Assay reproducibility.** Three aliquots of a serum sample from a with high TL melanoma patient and from a healthy donor were depleted and digested in parallel. Additionally, three aliquots of the same samples were digested without prior depletion. Triplicate LC-MS measurements were performed, resulting in a total of nine injections for each sample type. Box plots representing the CVs of peptide peak areas normalized to those of standard peptides are shown. No significant difference was observed between with high TL melanoma samples and healthy donor sample. The main variations seem not to be generated in the depletion step. In average, the median CV of the entire assay including depletion, digestion and variations of LC-MS measurements was less than 20%.

Figure S4. ICAM1 and CD163. The boxplots show the quantitative data for ICAM1 and CD136 from the MRM analysis of melanoma samples with low or high tumor load (TL). For both proteins a high fold change of 1.68 and 1.56 was observed. However, the respective p-value of 0.055 and 0.062 did not fulfill the applied criteria of a significant regulation with $p < 0.05$.

Table S1. Clinical parameters, as well as classification in low and high tumor load, for patients included in the present study.

Table S2. List of identified and MS1-based quantified proteins from the shotgun Orbitrap analysis using MaxQuant software tools.

Table S3. List of proteins, peptides and transitions of the finally scheduled MRM method.

Table S4. Results of the statistical analysis of MRM proteomics data.

Table S5. Quantification data generated from the statistical analysis of MRM proteomics data.

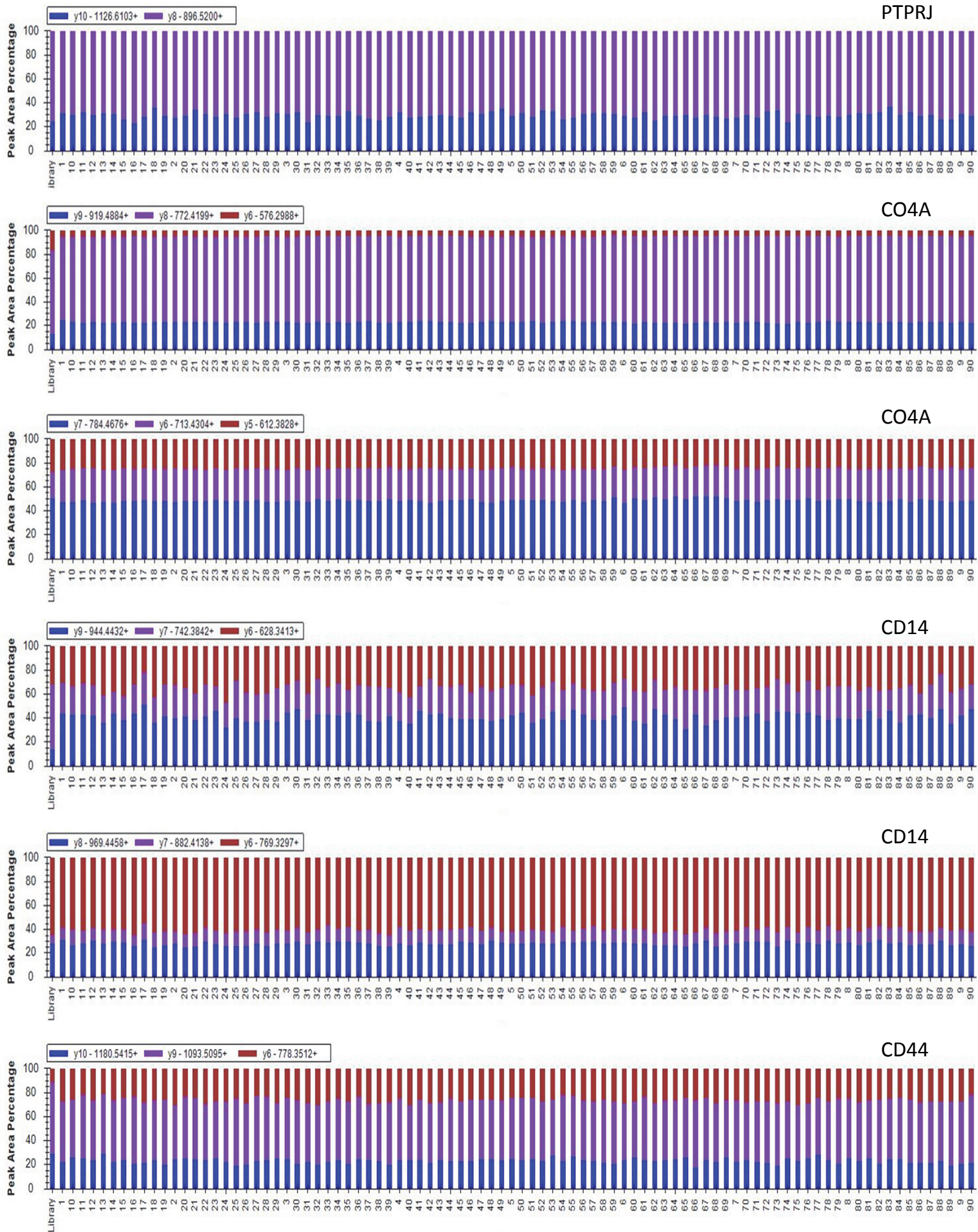


Figure S1

Run

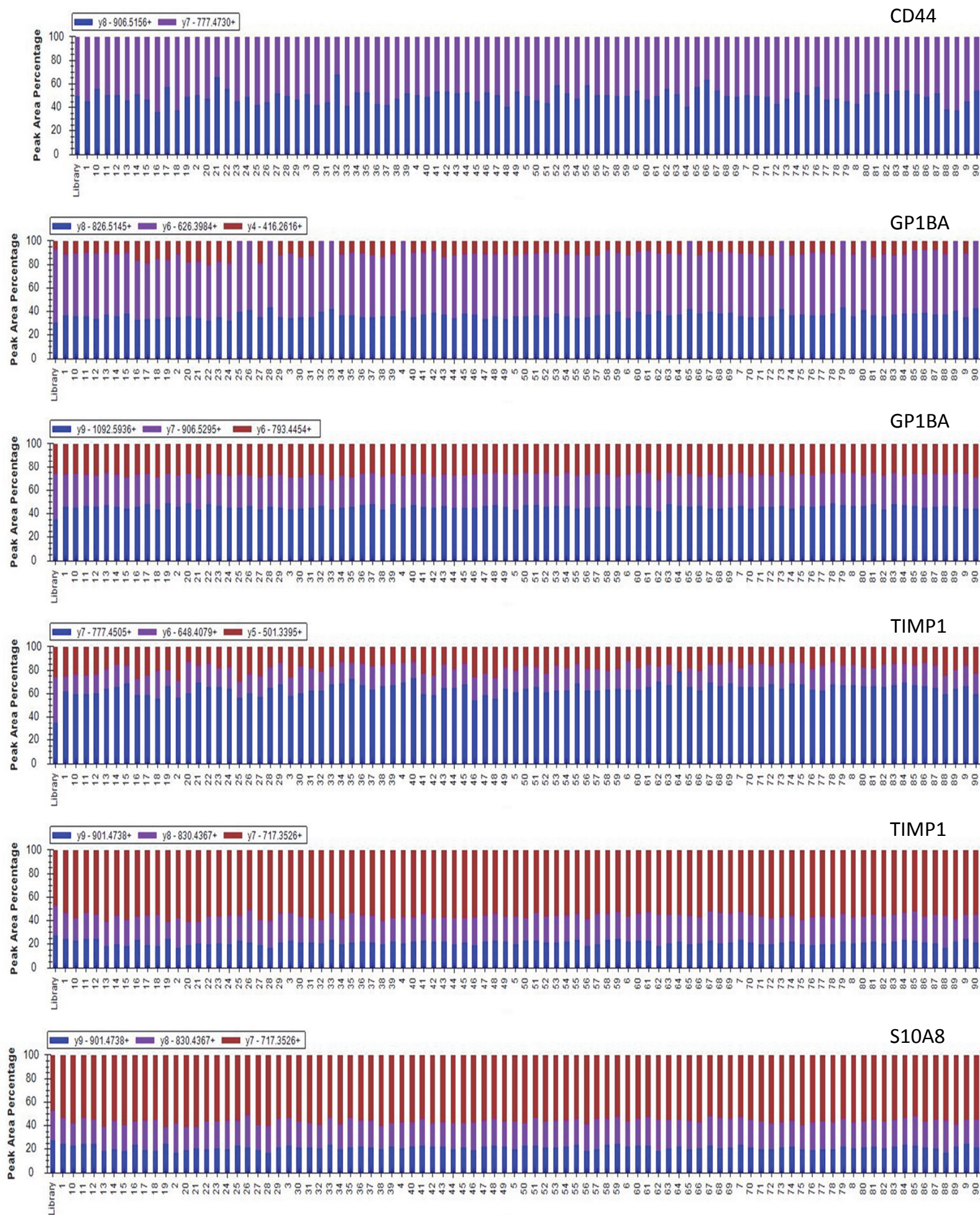


Figure S1

Run

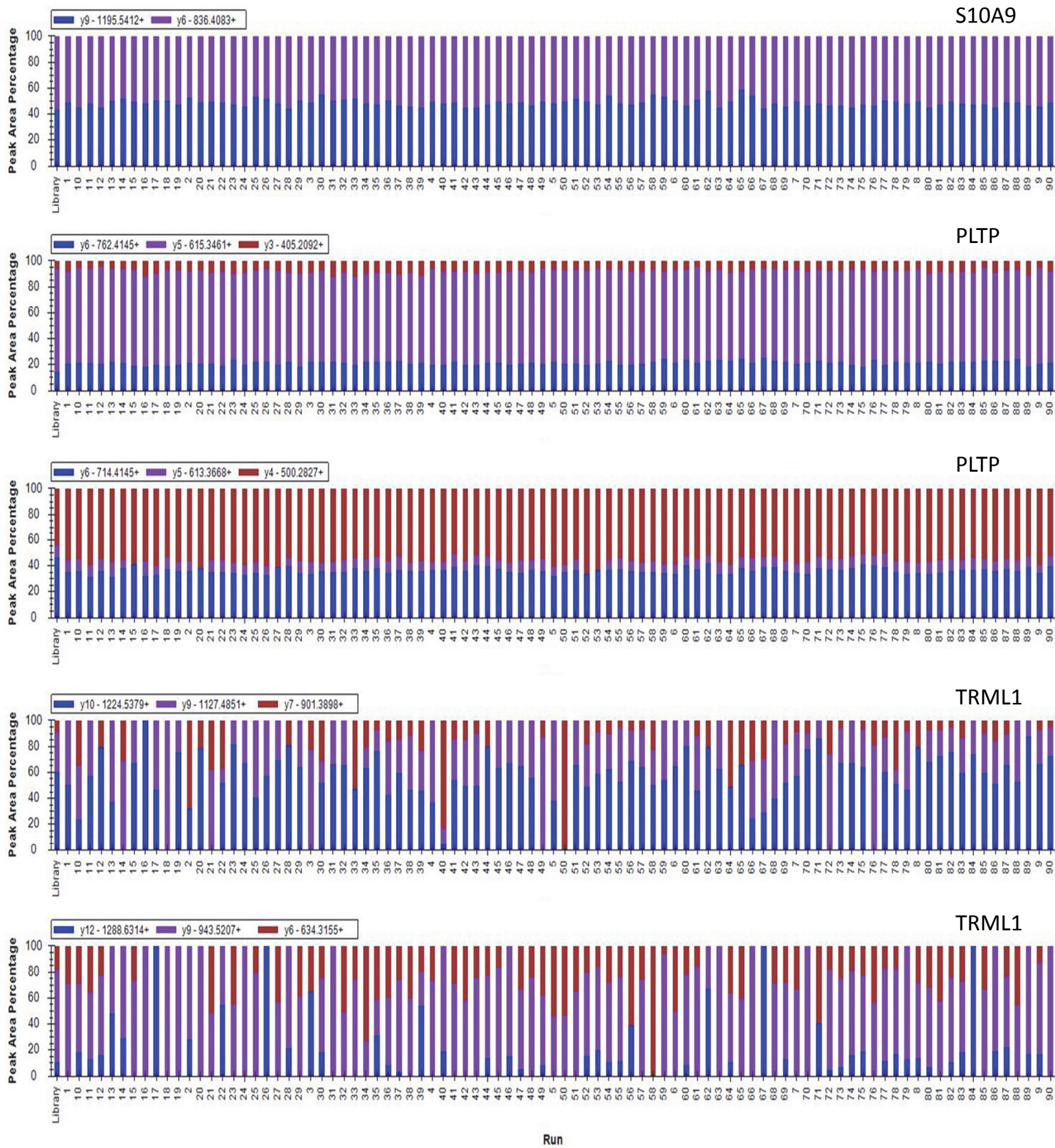
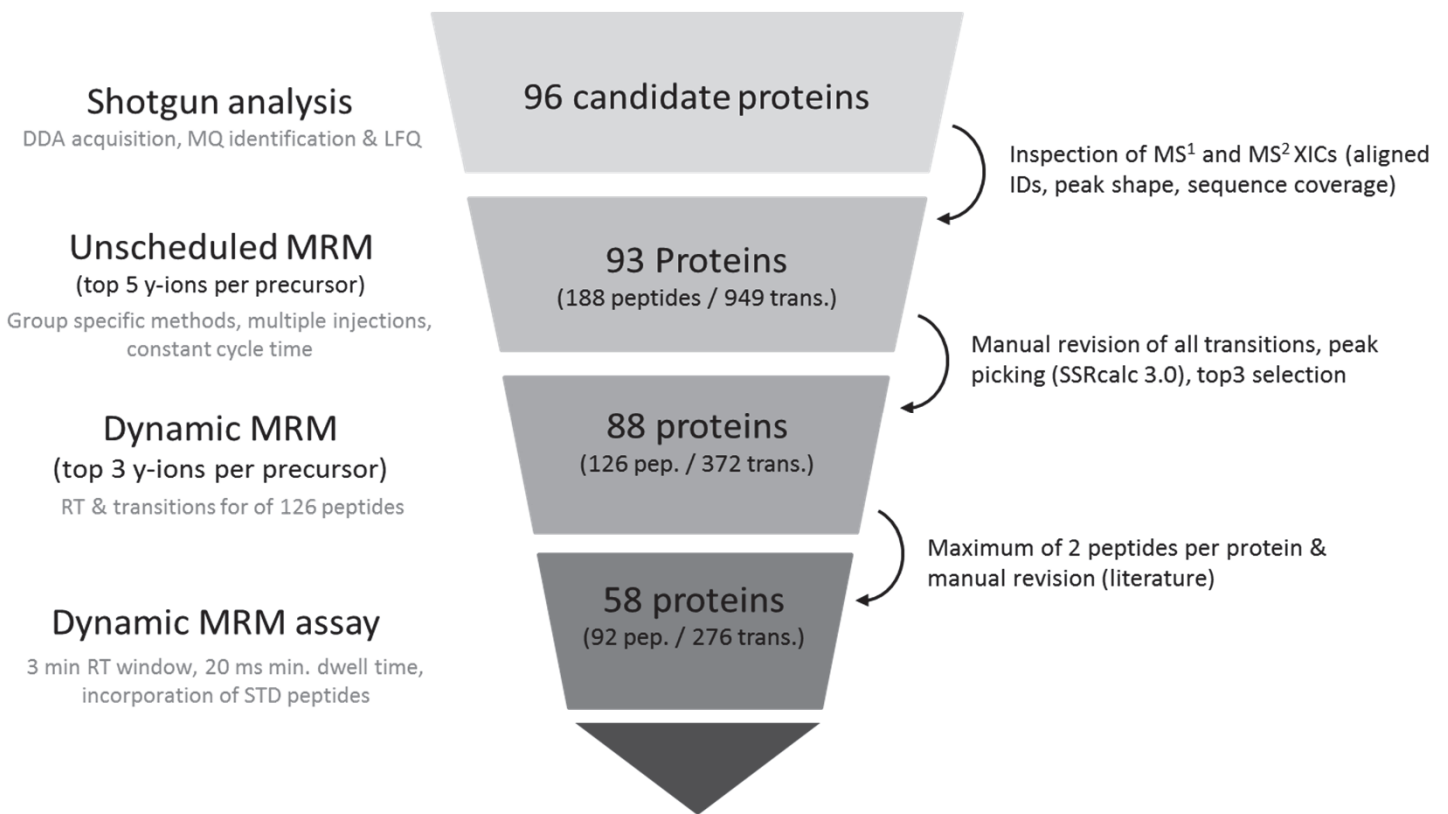


Figure S1



MRM Target Proteins		
4F2 cell-surface antigen heavy chain	Fibronectin	Neural cell adhesion molecule L1-like protein
Alpha-1-acid glycoprotein 1	Follistatin-related protein 1	Phospholipid transfer protein
Alpha-1-acid glycoprotein 2	Galectin-3-binding protein	Platelet glycoprotein Ib alpha chain
Aminopeptidase N	Gamma-glutamyl hydrolase	Proteasome subunit alpha type-6
Angiopoietin-related protein 3	Glutathione S-transferase omega-1	Protein S100-A8
Apolipoprotein A-IV	Glutathione synthetase	Protein S100-A9
Aspartate aminotransferase, cytoplasmic	Heparanase	Receptor-type tyrosine-protein phosphatase eta
Beta-Ala-His dipeptidase	Insulin-like growth factor-binding protein 2	Retinol-binding protein 4
Cadherin-2	Intercellular adhesion molecule 1	Scavenger receptor cysteine-rich type 1 protein M130
Calumenin	Lactate dehydrogenase A	Selenoprotein P
Cartilage acidic protein 1	L-lactate dehydrogenase B chain	Serum amyloid A-1 protein
Cathepsin D	L-selectin	Serum amyloid A-2 protein
CD44 antigen	Macrophage colony-stimulating factor 1 receptor	Serum amyloid P-component
Chondroitin sulfate proteoglycan 4	Macrophage mannose receptor 1	Tetranectin
Coagulation factor XIII A chain	Matrix metalloproteinase-9	Transforming growth factor-beta-induced protein ig-h3
Collectin-11	Melanocyte protein PMEL	Transthyretin
Complement C4-A	Membrane primary amine oxidase	Trem-like transcript 1 protein
Complement factor H-related protein 1	Metalloproteinase inhibitor 1	Tryptophan--trNA ligase, cytoplasmic
C-reactive protein	Monocyte differentiation antigen CD14	
Ferritin light chain	Neural cell adhesion molecule 1	

Figure S2

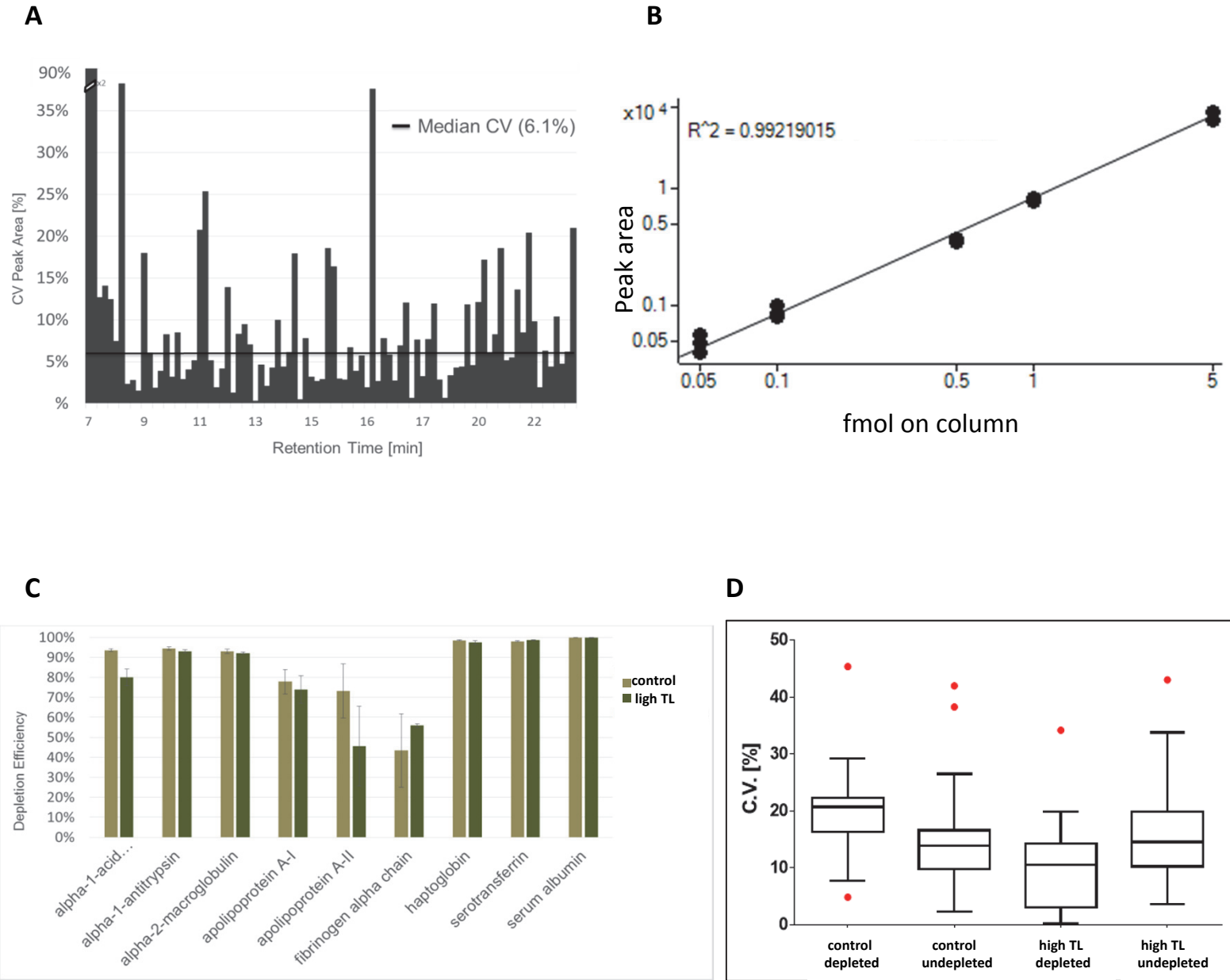


Figure S3

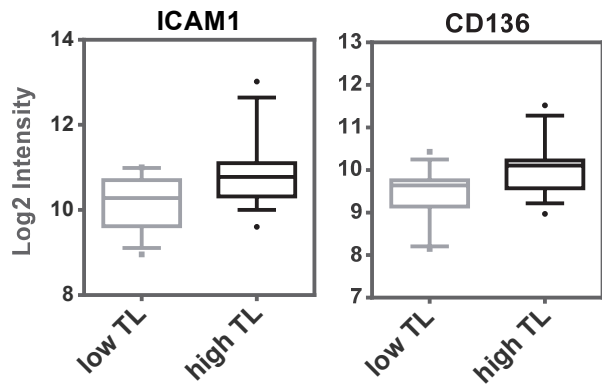


Figure S4